Journal Name

ARTICLE

Supporting Information

Missing-node directed synthesis of hierarchical pores on a zirconium metal-organic framework with tunable porosity and enhanced surface acidity *via* microdroplet flow reaction

Ying Wang,[a,b] Liangjun Li,[a] Pengcheng Dai,[a] Liting Yan,[a,b] Lei Cao,[a] Xin Gu,[a] and Xuebo Zhao[*a]

[a.] Research Centre of New Energy Science and Technology, Research Institute of Unconventional Oil & Gas and Renewable Energy, China University of Petroleum (East China), Qingdao, 266580, P. R. China.

[b.] College of Science, China University of Petroleum (East China), Qingdao, 266580, P. R. China.

[*] Email: zhaoxuebo@upc.edu.cn

S1. Infrared spectroscopy

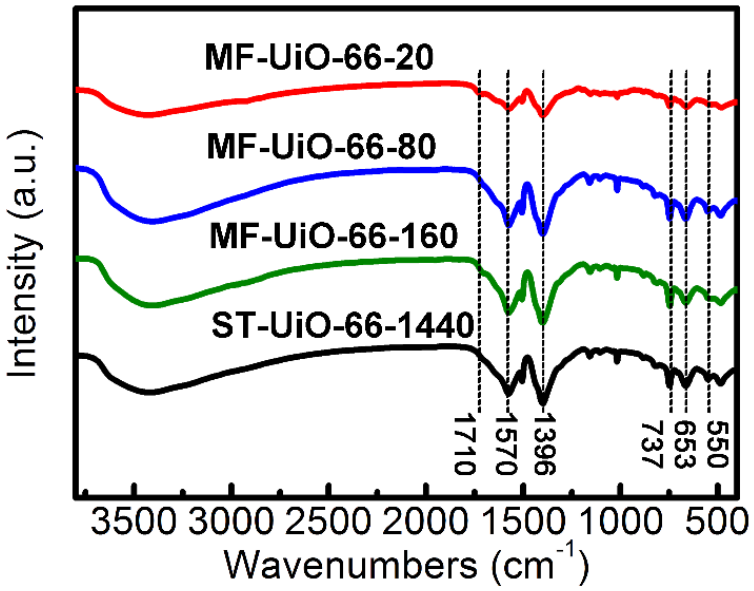

Figure S1. Comparison of infrared spectroscopy of the as synthesized sample of MF-UiO-66-20, MF-UiO-66-80, MF-UiO-66-160 and the sample obtained from solvothermal synthesis (ST-UiO-66-1440). The peaks at v = 1570 cm^{-1} and v = 1396 cm^{-1} are ascribed to the asymmetric stretching vibration and symmetrical stretching vibration of BDC^{2-}, respectively. The triplet at v = 737 cm^{-1}, v = 653 cm^{-1} and v = 550 cm^{-1} are attributed to Zr-O_2[1-3]. The weak peaks at v = 1710 cm^{-1} can be assigned to the coordinated-free COOH group (1690 cm^{-1}~ 1770 cm^{-1}).

S2. Pore structure parameters

Table S1. Pore structural parameters for MOFs synthesized by solvothermal and microdroplet synthesis.

MOFs	Residence time (min)	SBET ($m^2 \cdot g^{-1}$)	$V_{micro+meso}$ ($cm^3 \cdot g^{-1}$)	V_{micro} ($cm^3 \cdot g^{-1}$)	V_{meso} ($cm^3 \cdot g^{-1}$)	Meso-pore ratio (%)	References
MF-UiO-66-20	20	555	1.277	0.149	1.128	88.33	This work
MF-UiO-66-80	80	771	0.684	0.182	0.502	73.39	This work
MF-UiO-66-160	160	817	0.493	0.290	0.203	41.18	This work
ST-UiO-66-1440[a]	1440 [a]	1247	0.533	0.494	0.039	7.32	This work
UiO-66[4]	1440 [a]	1013	0.360	0.360	0	/	[4]

[a] The MOF was synthesized under solvothermal conditions for 24 hours.

S3. SEM and TEM photographs for ST-UiO-66-1440

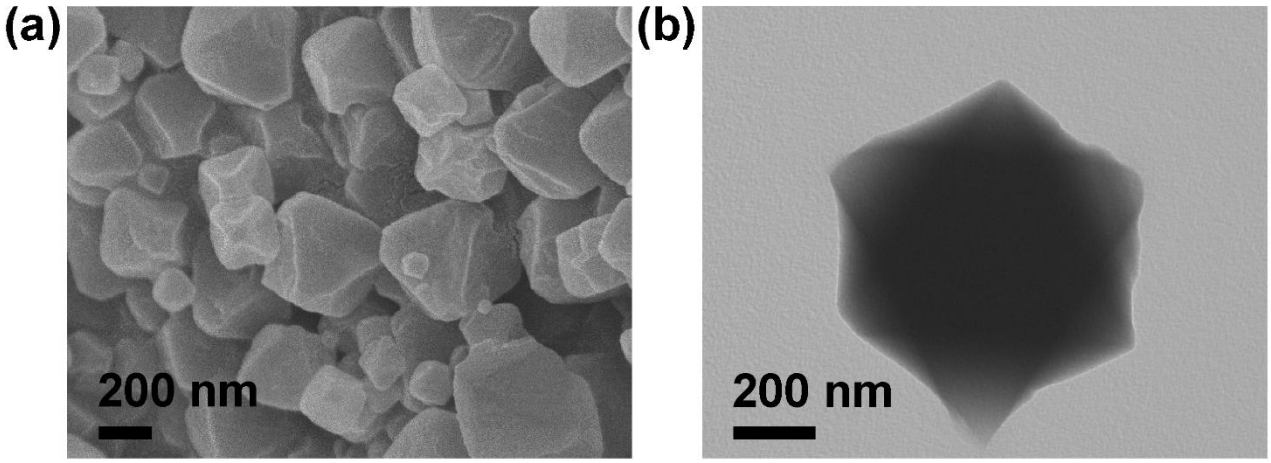

Figure S2. (a) SEM photograph for ST-UiO-66-1440; (b) TEM photograph for ST-UiO-66-1440.

S4. XPS spectra

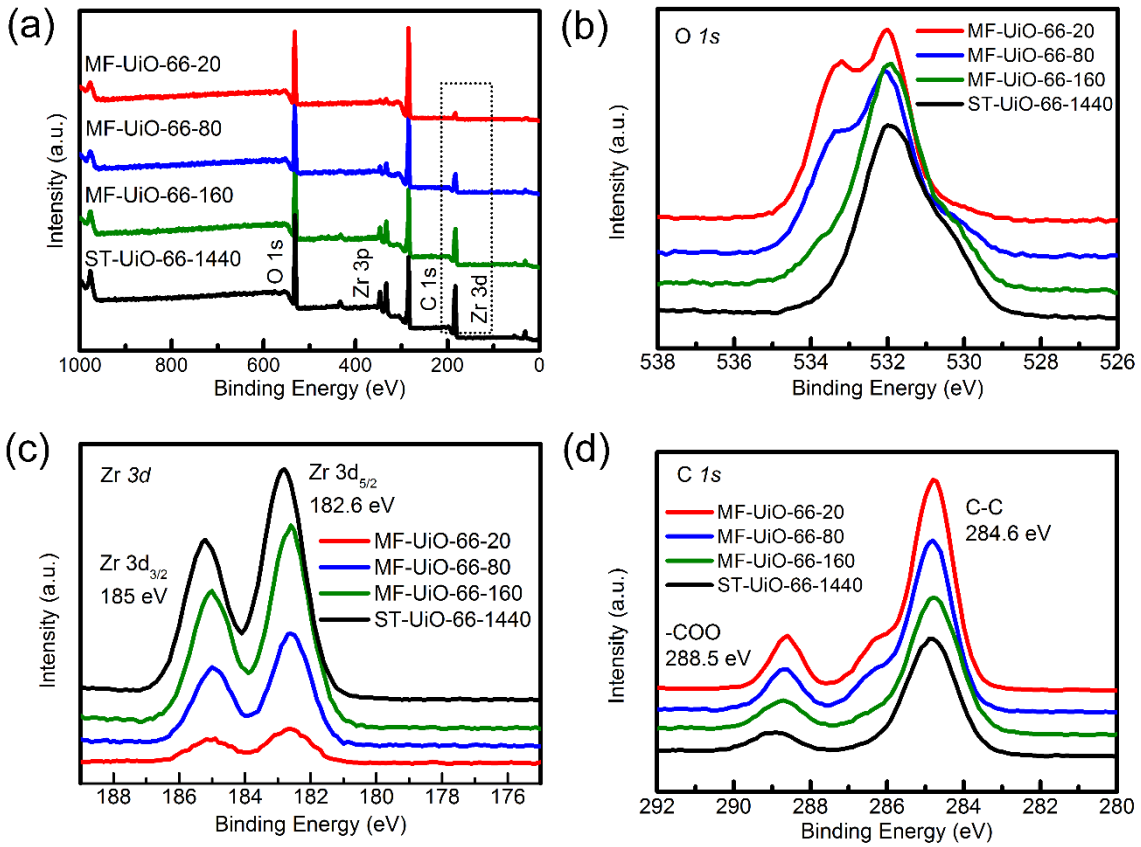

Figure S3. XPS spectra of (a) survey scan of MF-UiO-66-20, MF-UiO-66-80, MF-UiO-66-160 and ST-UiO-66-1440 and the narrow scan in the O *1s* (b), Zr *3d* (c) and C *1s* (d) of MF-UiO-66-20, MF-UiO-66-80, MF-UiO-66-160 and ST-UiO-66-1440, respectively.

Table S2. Spectral fitting parameters for MOFs synthesized by solvothermal and microdroplet flow-reaction synthesis.

MOFs	COOH (% Area)	Zr-O-Zr (% Area)	Zr-O-C (% Area)
MF-UiO-66-20	49.12	5.96	44.92
MF-UiO-66-80	40.13	11.70	48.18
MF-UiO-66-160	17.15	20.41	62.44
ST-UiO-66-1440[a]	5.40	24.98	69.63

[a] The MOF was synthesized under solvothermal conditions for 24 hours

S5. Correlation studies of pore structural parameters

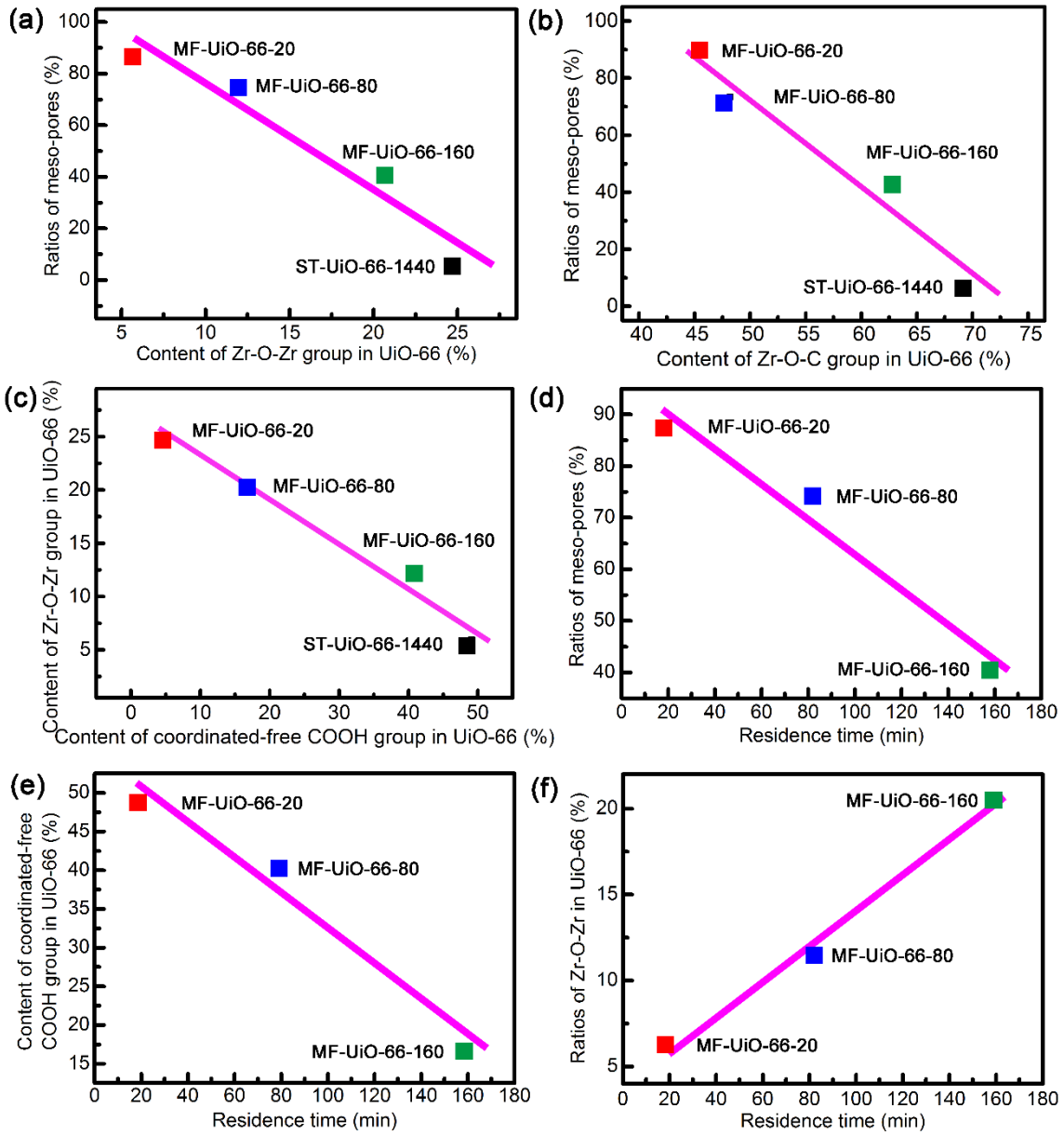

Figure S4. The fitted linear between the ratios of (a) mesopores and the content of Zr-O-Zr group; (b) the ratios of mesopores and the content of Zr-O-C group; (c) the content of Zr-O-Zr group and the content of coordinated-free COOH group; (d) the ratios of mesopores and residence time; (e) the content of coordinated-free COOH group and residence time; (f) the content of Zr-O-Zr group and residence time.

S6. ICP analysis

Table S3. The content of Zr in the MF-UiO-66-*t* and ST-UiO-66-1440 determined by ICP analyses.

MOFs	MF-UiO-66-20	MF-UiO-66-80	MF-UiO-66-160	ST-UiO-66-1440
Content of Zr (wt%)	20.16	23.15	25.46	29.89

S7. TGA analysis

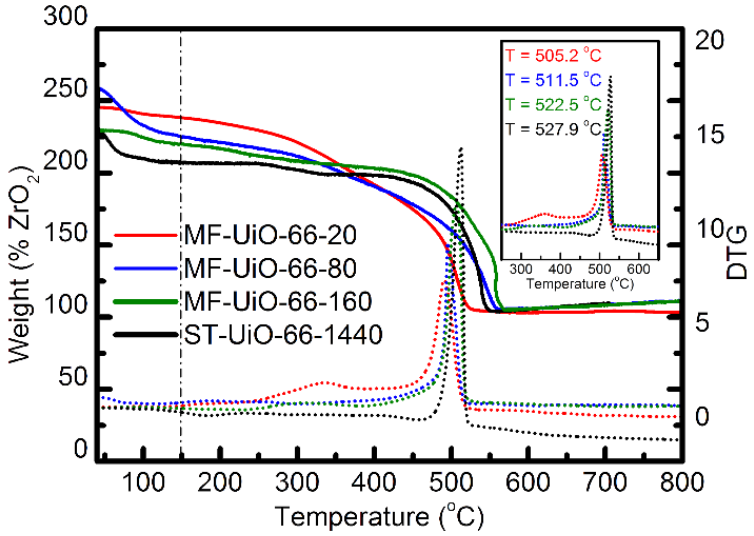

Figure S5. Thermo-gravimetric curve for MF-UiO-66-20 (red), MF-UiO-66-80 (blue), MF-UiO-66-160 (green) and ST-UiO-66-1440 (black) under air atmosphere. (Heating rate: 5 °C/min). All of these samples have been activated by Soxhlet extraction and vacuum drying at 120 °C.

Table S4. The estimated organic groups for these MOFs from TGA analyses.

MOFs	Decomposition Starting Point (relative to ZrO_2)		Weight loss (relative to ZrO_2)
	Theoretical	Experimental	
MF-UiO-66-20		240.9	140.9
MF-UiO-66-80		225.4	125.4
MF-UiO-66-160		220.8	120.8
ST-UiO-66-1440[a]	220.2[5]	207.5	107.5

[a] The MOF was synthesized under solvothermal conditions for 24 hours

S8. PXRD of MF-UiO-66-80 at different temperature

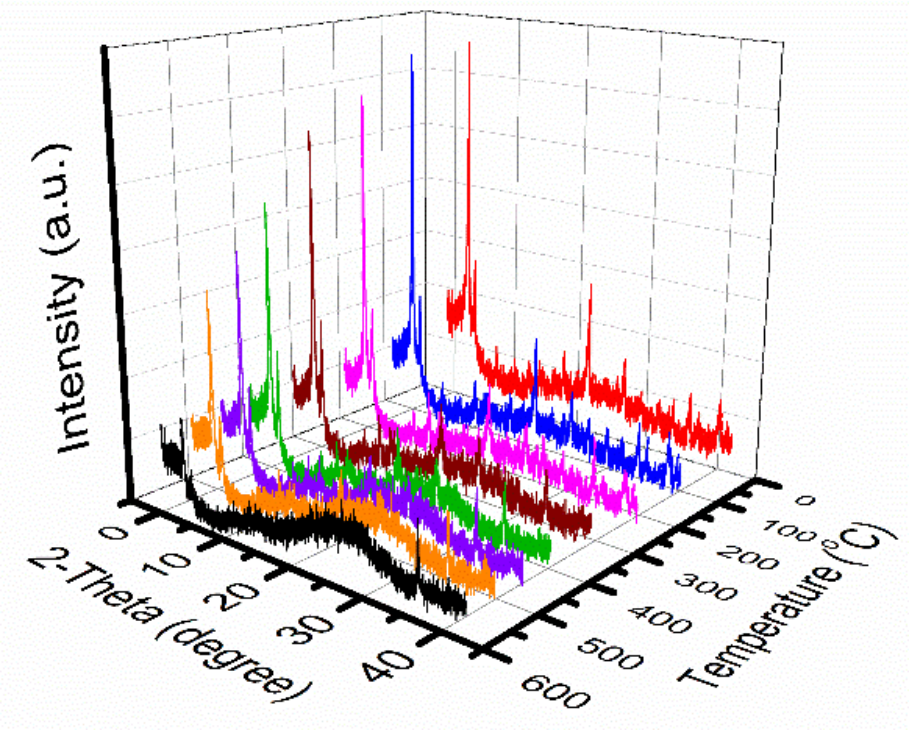

Figure S6. The in-situ temperature-resolved PXRD pattern of MF-UiO-66-80 in different temperature range of 25-550 °C

S9. Water stability

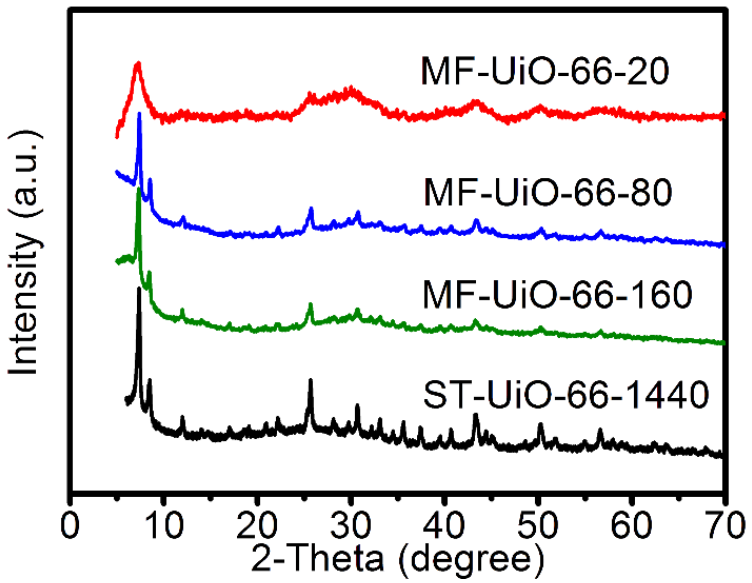

Figure S7. PXRD patterns of these MOFs treated by soaking in the boiling water for 24 hours.

S10. Acidity measurements

Table S5. The determination of pH for MOFs synthesized by solvothermal and microdroplet flow-reaction synthesis.

MOFs	pH value Soaking time (2 h)	pH value Soaking time (12 h)	pH value Soaking time (24 h)	pH value Soaking time (168 h)
MF-UiO-66-20	3.23	3.27	3.21	3.18
MF-UiO-66-80	3.31	3.43	3.38	3.28
MF-UiO-66-160	3.88	4.06	3.75	3.54
ST-UiO-66-1440[a]	4.94	5.13	5.15	4.74
Deionized water	6.85	6.48	6.86	6.80

[a] The MOF was synthesized under solvothermal conditions for 24 hours.

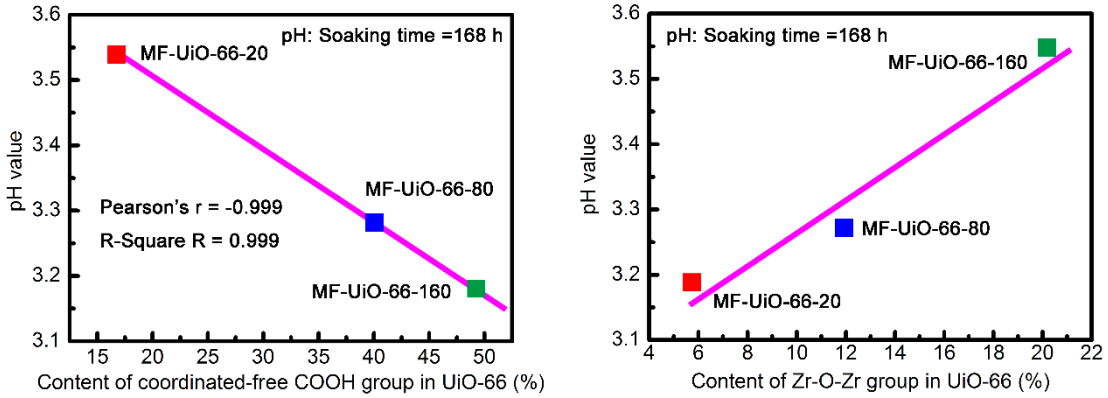

Figure S8. (a) The trend of the pH value with the content of coordinated-free COOH group and (b) the trend of the pH value with the content of Zr-O-Zr group.

S11. Gas adsorption isotherms on MF-UiO-66-20 and ST-UiO-66-1440

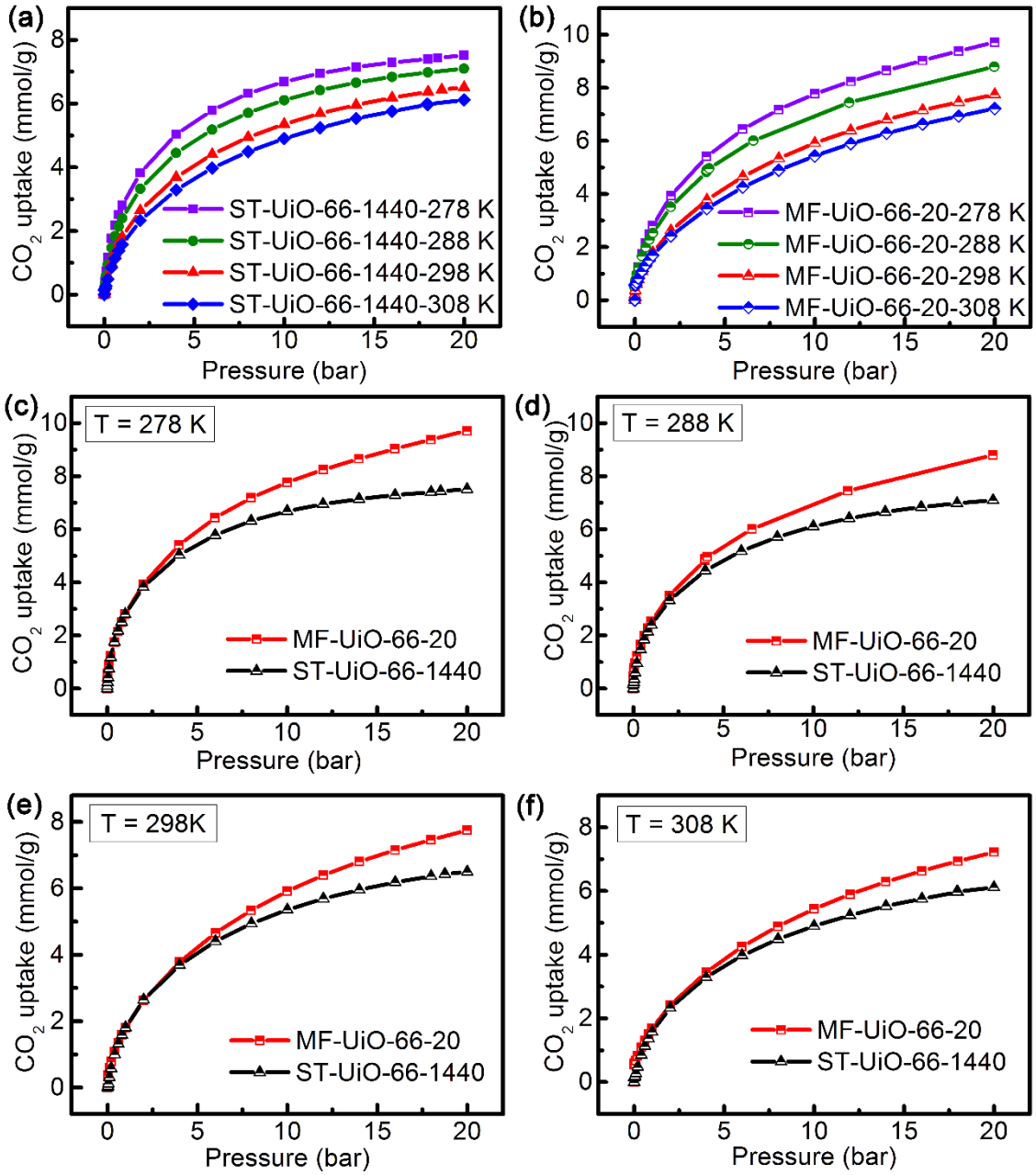

Figure S9. Adsorption isotherms of CO_2 on ST-UiO-66-1440 and MF-UiO-66-20 at 278 K, 288 K, 298 K and 308 K.

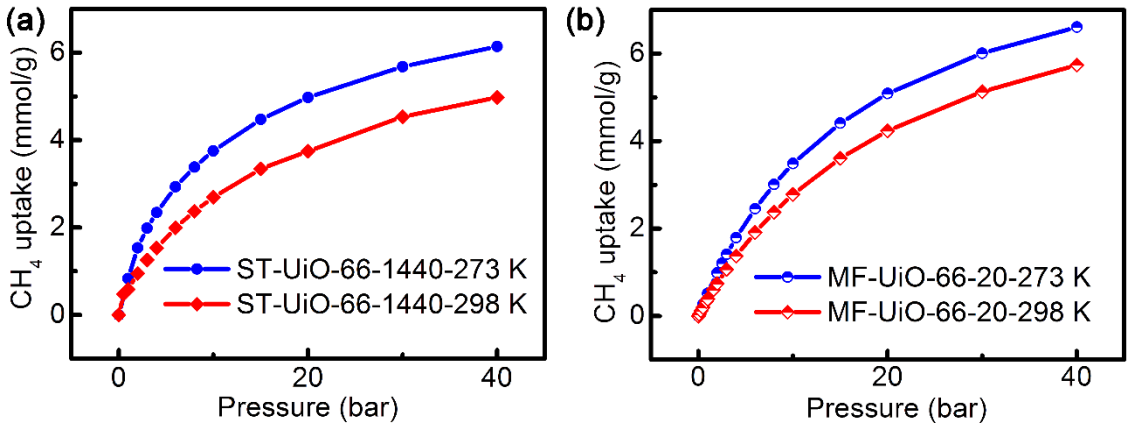

Figure S10. Adsorption isotherms of CH_4 on ST-UiO-66-1440 and MF-UiO-66-20 at 273 K and 298 K.

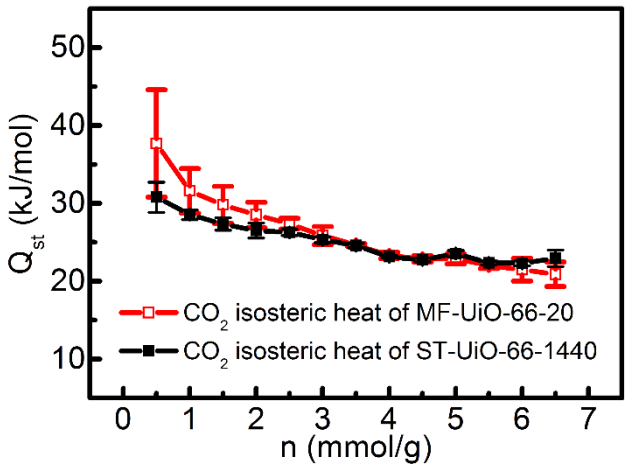

Figure S11. The variation of Q_{st} on ST-UiO-66-1440 and MF-UiO-66-20 with amount adsorbed for CO_2.

S12. The repeated synthesis of MF-UiO-66-20 and MF-UiO-66-80

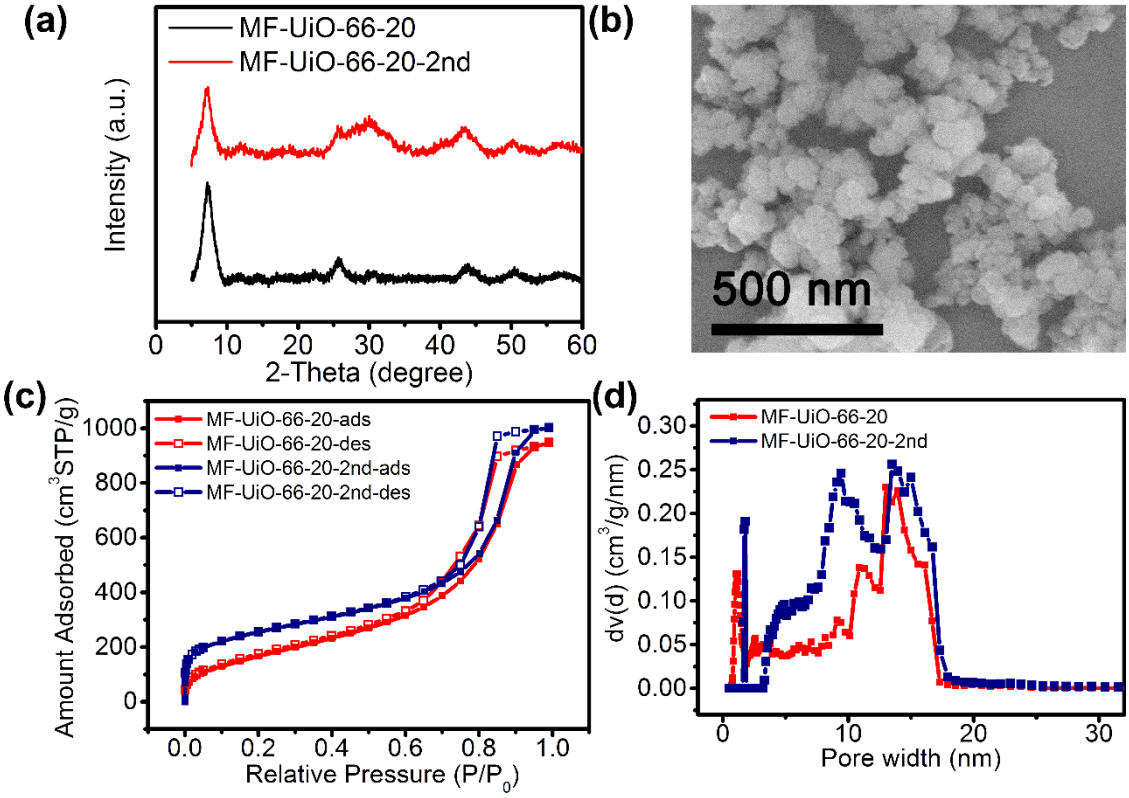

Figure S12. (a) XRD patterns of MF-UiO-66-20 and MF-UiO-66-20-2nd; (b) SEM photograph for MF-UiO-66-20 and MF-UiO-66-20-2nd; (c) N_2 isotherms at 77 K for MF-UiO-66-20 and MF-UiO-66-20-2nd; (d) The pore size distribution for MF-UiO-66-20 and MF-UiO-66-20-2nd.

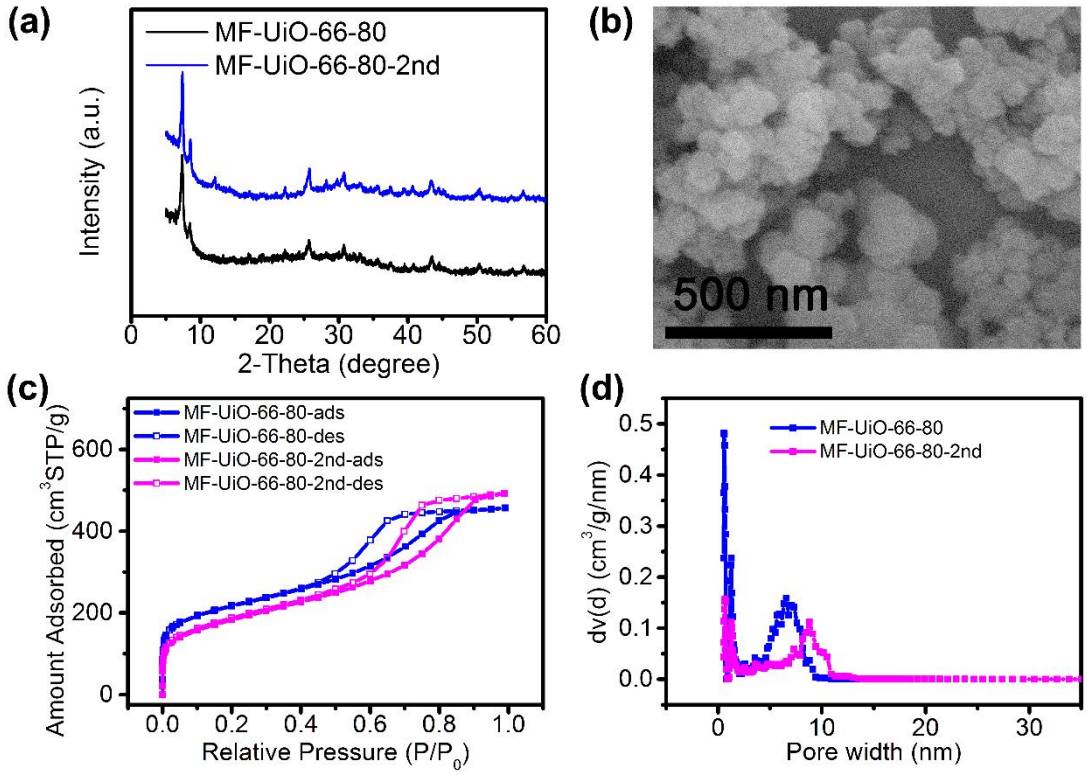

Figure S13. (a) XRD patterns of MF-UiO-66-80 and MF-UiO-66-80-2nd; (b) SEM photograph for MF-UiO-66-80 and MF-UiO-66-80-2nd; (c) N_2 isotherms at 77 K for MF-UiO-66-80 and MF-UiO-66-80-2nd; (d) The pore size distribution for MF-UiO-66-80 and MF-UiO-66-80-2nd.

References

1. X. Zhu, J. Gu, Y. Wang, B. Li, Y. Li, W. Zhao and J. Shi, *Chem. Commun.*, 2014, **50**, 8779-8782.
2. M. Kandiah, S. Usseglio, S. Svelle, U. Olsbye, K. P. Lillerud and M. Tilset, *J. Mater. Chem.*, 2010, **20**, 9848-9851.
3. S. Chavan, J. G. Vitillo, D. Gianolio, O. Zavorotynska, B. Civalleri, S. Jakobsen, M. H. Nilsen, L. Valenzano, C. Lamberti, K. P. Lillerud and S. Bordiga, *Phys. Chem. Chem. Phys.*, 2012, **14**, 1614-1626.
4. J. H. Cavka, S. Jakobsen, U. Olsbye, N. Guillou, C. Lamberti, S. Bordiga and K. P. Lillerud, *J. Am. Chem. Soc.*, 2008, **130**, 13850-13851.
5. G. C. Shearer, S. Chavan, S. Bordiga, S. Svelle, U. Olsbye and K. P. Lillerud, *Chem. Mater.*, 2016, **28**, 3749-3761.